Prog. Oceanog. Vol. 14, pp. 231–257, 1985.
Printed in Great Britain.

0079-6611/85 $0.00 + .50

Currents, Fronts and Eddy Fluxes in the Canary Basin

R. H. KÄSE,* W. ZENK,* T. B. SANFORD† and W. HILLER‡

*Institut für Meereskunde an der Universität Kiel, Düsternbrooker Weg 20, 2300 Kiel 1, F.R.G.
†Applied Physics Laboratory and School of Oceanography, University of Washington, Seattle, WA 98105, U.S.A.
‡Alfred-Wegener-Institut für Polarforschung, Columbus-Center, 2850 Bremerhaven, F.R.G.

Abstract – Hydrographic data from two cruises in the Canary Basin (*Meteor* 57, July 1981; *Poseidon* 86, April 1982) are analysed with respect to current distribution and lateral heat flux in the Azores–Madeira region.

The first part of the data base consists of long transects of XBT and G.E.K. measurements between Cape Finisterre (North West Spain) and the northern Canary Basin, where several year-long current meter records exist. Further information is obtained by thermosalinograph surface data and by expendable current profilers (XCP). Geostrophic currents are derived from XBT profiles, using the tight temperature–salinity relationship in the depth range of the *Warmwassersphäre*. The results compare well with the G.E.K. and XCP current observations. The second part consists of CTD data from an eddy resolving, box-shaped CTD survey ($500 \times 500\,km^2$) centered at the mooring location (33°N, 22°W). The observations are supplemented by satellite-buoy trajectories. Horizontal parameter distribution is shown in terms of objectively contoured maps.

Bands of spatially enhanced energetic structures, seen in the long transects are further resolved by the box survey as a deep jet-like current system cross the Canary Basin in a west–east direction. Associated with this Azores Current is a frontal zone with near-surface temperature and salinity steps of order 2 K and 0.3 practical salinity units.

The dynamic topography field can be decomposed into a linear background field, a Rossby wave and a mesoscale eddy field. We find that major contributions to the meridional eddy heat flux are confined to the vicinity of the Azores current frontal zone. It is shown that the principal balance in the temperature equation is between heating by the mean horizontal advection terms and cooling by the eddy flux divergence.

1. INTRODUCTION

HEAT flux in the ocean is a subject of considerable scientific importance in studies of global and regional climate. Heat absorbed in the tropical latitudes is transported meridionally (and zonally) in the ocean to higher latitudes. The influence of this heat on subpolar regions is well recognized. The modes of meridional heat transport in the North Atlantic have been made clearer by the analyses of BRYDEN and HALL (1980) and HALL and BRYDEN (1982). They report that most of the heat is transported northward by the Florida Current with smaller contributions from baroclinic and Ekman flows. One possible contribution which is estimated to be small and usually ignored is the open ocean eddy transport of heat. It is true, however, that the role and importance of eddy processes in the lateral transport are ill-resolved and largely uncertain.

In this paper we report observations of spatial mean and eddy variability in the Canary Basin and compare these results with a simple heat balance model. The lack of sufficient information on the eddy processes is due in large measure to the difficulties in making adequate

measurements. Quite often the eddy flux results from rather small correlations between large signals, and thus it is hard to obtain estimates with sufficient statistical significance. We have overcome the sampling problem by obtaining long transects of XBT and geomagnetic electrokinetograph (G.E.K.) measurements, several-year-long moored current meter observations and a high-resolution density survey. These independent measurements all reveal a consistent picture of the eddy processes in this area.

The eastern North Atlantic is a region of low eddy activity. DANTZLER (1977), WYRTKI *et al.* (1976) and recently EMERY (1983) analyzed the eddy potential and kinetic energies for the North Atlantic and found a minimum in both quantities in the eastern part of the subtropical gyre. Therefore it seems reasonable that this should be an area of small eddy heat transport since that is proportional to the product of small velocity and temperature perturbations. Not only are the component variables, v and T, small but previous investigations have found small vT correlations. For example, WUNSCH (1980) reports an eddy correlation between v and T of about 0.04 at 40°N. Our observations reveal unexpectedly large eddy temperature fluxes that do not result from higher eddy energies but from larger eddy correlations. Eddy correlations of 0.25 on average are observed in our surveys.

The eastern basin is a region where the mean circulation is thought to be governed by Sverdrup dynamics (LEETMAA, NIILER and STOMMEL, 1977). The conventional picture is of weak meridional flow with small zonal components. The classic description of the property fields in this area is that of WUST (1935). He noted that the density distribution at the 200 m level was representative of the upper ocean circulation. His 200 m chart, shown in Fig. 1 (Fig. 47, p. 107, Emery trans.), depicts a Sverdrup-like, meridional flow south of 30°N and a

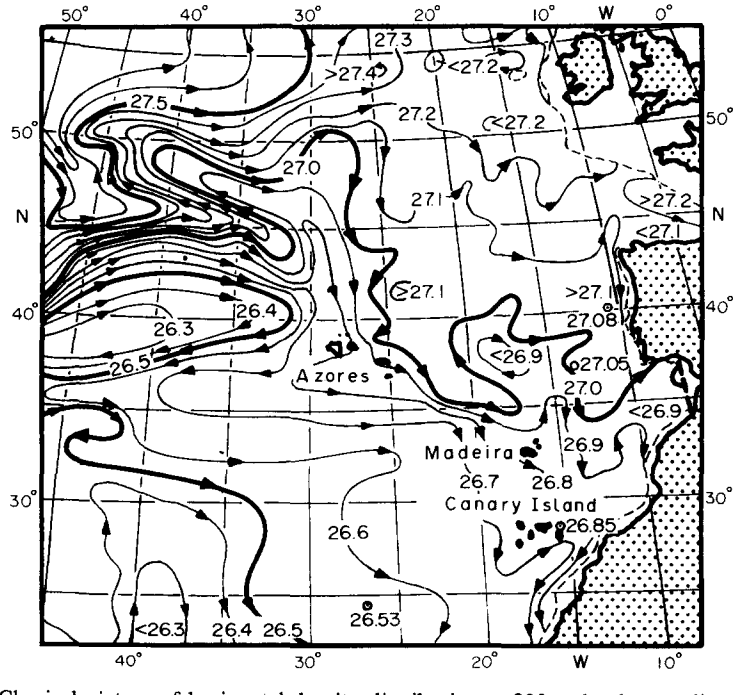

FIG. 1. Classical picture of horizontal density distribution at 200 m depth according to WÜST (1935).

strong zonal flow north of this latitude in the vicinity of the Azores and Madeira. This current is depicted as a zonal, but wider flow in the dynamic topography charts of LEETMAA, NIILER and STOMMEL (1977). We call this flow the Azores Current as it is labeled in the international sea chart no. 105. (Service hydrographique et oceanographique de la marine, Brest, 1978).

This paper is structured as follows: In Section 2 we give a short outline of the cruises *Meteor* 57 and *Poseidon* 86 and the methods used. In Section 3 we present two long sections as a background against which the three dimensional CTD survey in the central Canary Basin was conducted. The analysis is given in Section 4. We show the existence of a highly energetic zone southeasterly of the Azores which contributes significantly to the northward eddy flux as part of the local temperature balance, presented in Section 5. In the concluding Section 6 we discuss the relevance of our results with respect to the gyre-scale circulation and propose a possible future observation strategy.

2. FIELD EXPERIMENTS

The majority of previous observations in the eastern North Atlantic is concentrated on hydrographic stations on mainly zonal or meridional sections. From these data the general upper ocean circulation pattern has been determined (DEFANT, 1961; WUNSCH and GRANT, 1982). Such data have generally been taken with station spacings of more than 100 km which are not uniformly distributed. In particular, the bulk of the more recent data has been obtained on zonal sections, while more of the earlier sections were meridional. For the present study the goal was to obtain a synoptic, box-shaped survey with spatial resolution of 55 km comparable with the Rossby radius of deformation (45 km). Moreover, new methods were employed to obtain finer-scale measurements, especially from a ship underway.

As a component of the research programme "Warmwassersphäre" of Kiel University two cruises were made to the vicinity of the Canaries–Azores. In addition to the cruises there were three moorings deployed in the area (MÜLLER and ZENK, 1983). Figure 2 depicts the station patterns for the *Meteor* 57 and *Poseidon* 86 cruises and the location of the central mooring.

On *Meteor* cruise 57, lasting from 16–31 July 1981, several methods of underway measurements were used (SANFORD and SPAIN, 1982). The track was subdivided into four legs. The first leg included all data recorded until the ship entered water deeper than 3,000 m on the western end of the English Channel. The second was between the English Channel and Cape Finisterre, while the third and longest extended from the latter to the Canary Islands. The fourth was between the Canary Islands and the Azores. Note that in this paper we only rely on data collected during leg 3 and leg 4.

During the whole cruise surface temperature and salinity measurements were obtained, and baroclinic surface flow (normal to the cruise track) was measured with a G.E.K. The *T/S* surface data were checked regularly by bucket temperature and salinity samples. All salinity data of this paper are given in practical salinity units. Usage of bathythermographs (XBT) provided a record of subsurface temperature structure, and occasional usage of expendable current profilers, XCP (SANFORD, DREVER, DUNLAP and D'ARARO, 1982), provided measurements of the subsurface velocity structure.

Poseidon 86 conducted a grid-pattern, upper-ocean CTD survey with a nominal spacing of 30 nautical miles during the period 28 March–13 April 1982 (KÄSE and RATHLEV, 1982). Online CTD data processing allowed for the adjustment of the station pattern in response to the observed structure of the density field. Specifically, stations in the southern, more quiescent region, were widely spaced, but those in the vicinity of a jet-like flow in the north were more

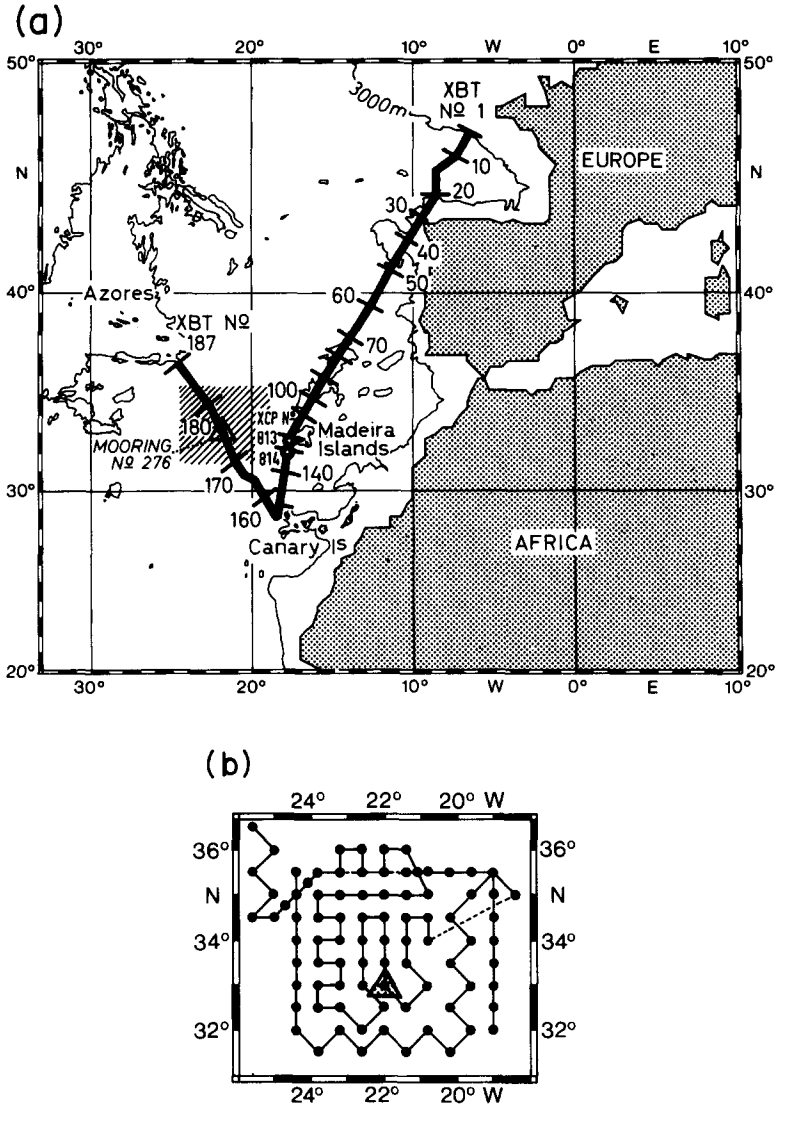

FIG. 2. Mooring locations and station patterns of *Meteor* 57 cruise, 16.7.–31.7.1981 (a), and *Poseidon* 86 CTD-survey, 28.3.–13.4.1982 (b). Large numerals denote XBT, small numerals XCP drop sites. The *Meteor* 57 cruise track was subdivided into leg 2: 47.5°N 6.5°W to 41.5°N 11°W, leg 3: 41.5°N 11°W to 29°N 18.5°W and leg 4: 29°N 18.5°W to 37.5°N 25.5°W.

closely spaced. The pattern of stations in Fig. 2(b) reflects this strategy. During this cruise all directly measured conductivity, temperature and pressure data (CTD) were obtained by the Kiel Multisonde of the Institute for Applied Physics of Kiel University (KROEBEL, 1973; KÄSE and RATHLEV, 1982). A further component of the *Poseidon* 86 data set was given by a cluster of 9 satellite tracked drifters (KRAUSS and KÄSE, 1984). In the analysis of the CTD and drifter data sets optimal estimation technique (HILLER and KÄSE, 1983) was used.

3. EASTERN NORTH ATLANTIC VARIABILITY

Attracted by the higher levels of mean and eddy kinetic energy, oceanographers have devoted considerable attention to the western basin of the North Atlantic while the eastern basin has not been investigated as much in the past few decades. This section will describe some of the new observations obtained on *Meteor* 57 in the eastern North Atlantic and discuss aspects of the large-scale nature of the flow and property distributions.

Hourly and bi-hourly XBT profiles are the principal source of subsurface temperature information. In addition we have used expendable current profilers (XCP). This device determines the vertical profile of temperature and of horizontal electric current between the surface and about 900 m. The current is interpreted in terms of velocity of the ocean required to produce the observed electric response through induction in the earth's magnetic field (DREVER and SANFORD, 1980). Each profile is of relative velocity, there being an unknown, depth-independent offset present (SANFORD, DREVER, DUNLAP and D'ARARO, 1982).

A saltbridge G.E.K. (MANGELSDORF, 1962) was deployed continuously during *Meteor* 57. The unique feature of this instrument, in contrast to the classic G.E.K. (VON ARX, 1950) is, that it is not necessary to reverse the ship's heading to determine the electrode offset. The G.E.K. velocity is related to the difference between the surface velocity and the conductivity-weighted vertically averaged velocity $\bar{v}^*$ (SANFORD, 1971). The G.E.K. is insensitive, therefore, to the barotropic velocity field. In this sense the motionally induced voltages on the G.E.K. equipment yield a velocity component that is similar to velocities derived from geopotential anomalies.

Such anomalies have been calculated through the use of averaged T/S relationship of STRAMMA (1981). The reliability of these geopotential anomalies depend critically on the tightness of the T/S relation as discussed by STRAMMA (1981). Uncertainties must be expected in the surface mixed layer and under the influence of the Mediterranean Water with its intermittency (EMERY and DEWAR, 1982).

Comparisons with XCP/XBT inferred velocities will be given next in combination with the geographical discussion of the long sections of *Meteor* 57.

XBT stations are indicated in Fig. 2(a). Isotherms together with the bottom topography and the surface T/S parameters are presented for legs 3 and 4 in Figs 3 and 4. Through the Canary Basin up to the Iberian Penninsula (leg 3, XBT Nr. $\geqslant 50$) the surface T/S data are rather well correlated. This behavior is indicative of the tight T/S relationship that one encounters in the intermediate layers of the warm water sphere of this open ocean region. Approaching the outer shelf toward Cape Finisterre, however, we observe pronounced fluctuations of the surface temperature. They probably are caused by coastal upwelling and a warm current along the Northern coast of Spain, which is seen in the G.E.K. record (SANFORD and SPAIN, 1982). In contrast to the temperature signal the salinity record barely shows variations ($\leqslant 0.1$) in the outer shelf region off Cape Finisterre and the Bay of Biscay.

The isotherms tend to descend to the south of Cape Finisterre with the 12°C isotherm being the first to deepen. The 12°C isotherm is at a depth of 100 m in the north and resides at 500 m in the south. The horizontal temperature gradient at any depth is small north of Cape Finisterre and south of Madeira. Two cold, low salinity pools of water are observed. The first is in the vicinity of the Josephine Bank and the second is found slightly south of Madeira. Just before reaching the Canary Islands a sharp rise in the isotherms occurs, indicating the presence of a strong current just west of the islands. Another notable feature is the spreading of the 17° and 18°C isotherms south of Madeira. This water type has its surface outcropping in the region of the Canary Basin and the subtropical front (cf. SARMIENTO, ROOTH and ROETHER, 1982).

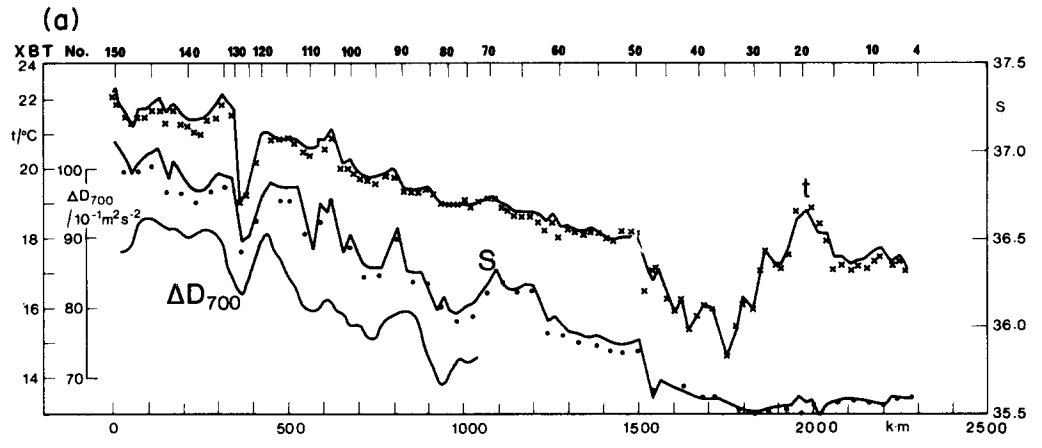

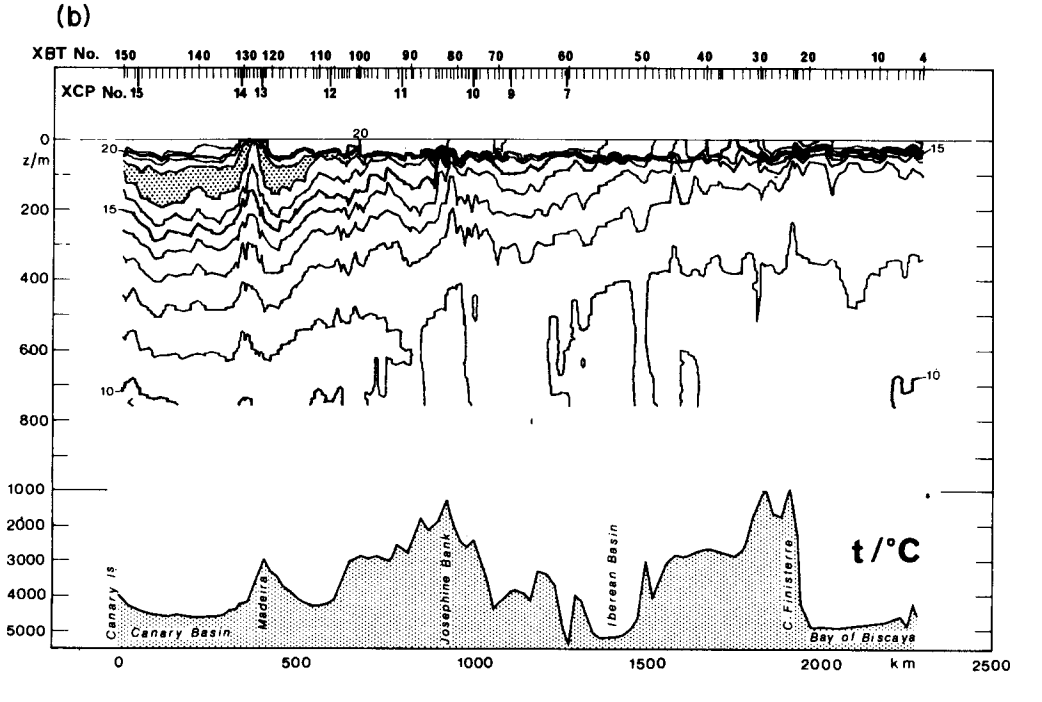

FIG. 3(a). Surface *T/S* parameters obtained with a thermosalinograph during the *Meteor* 57 cruise (47.5°N 6.5°W to 29°N 18.5°W) with checkvalues provided by bucket temperature (x) and salinity samples (·), and XBT derived geopotential anomalies relative to 700 m inferred from a mean *T/S* relationship.

FIG. 3(b). Subsurface temperature structure and bottom topography of *Meteor* 57 cruise obtained by XBT and XCP profiles. Note the spreading of the 17° and 18°C isotherms south of Madeira (dotted area) and the doming of the isotherms near Madeira connected with a strong cyclonic feature observed in the G.E.K. velocity (Fig. 5).

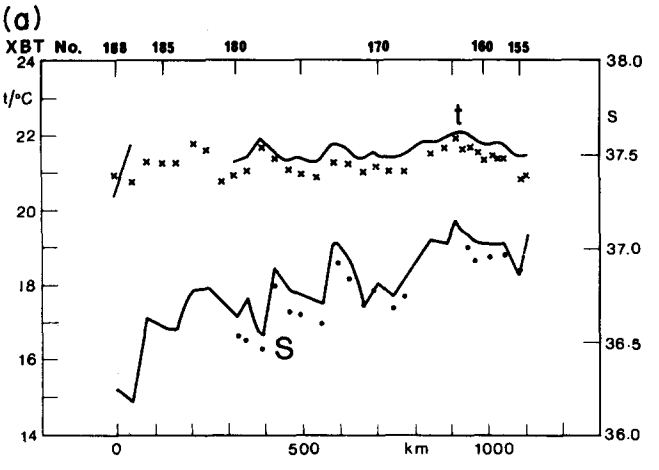

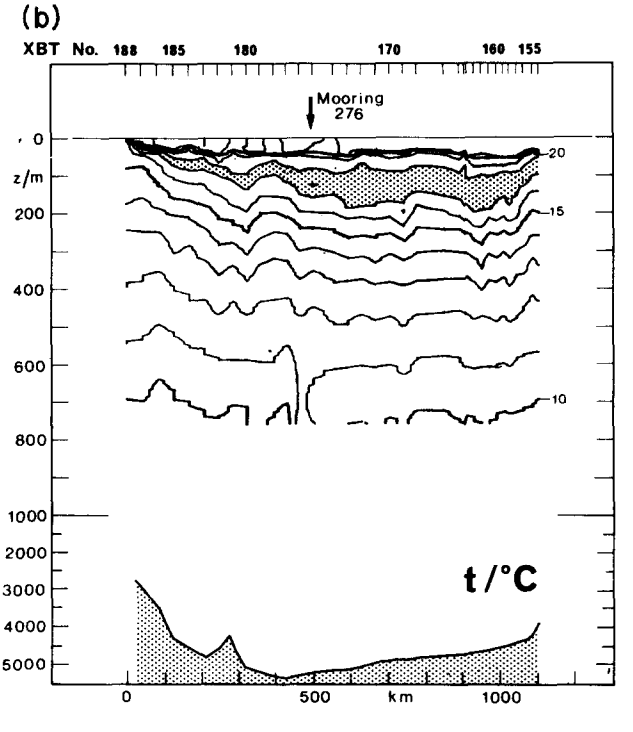

FIG. 4(a). Surface *T/S* parameters obtained with a thermosalinograph during the *Meteor* 57 cruise (29°N 18.5°W to 37.5°N 25.5°W) with checkvalues provided by bucket temperature (x) and salinity samples (·).

FIG. 4(b). Subsurface temperature structure and bottom topography of *Meteor* 57 cruise obtained by XBT and XCP profiles. The dotted area shows the spreading of the 17° and 18°C isotherms.

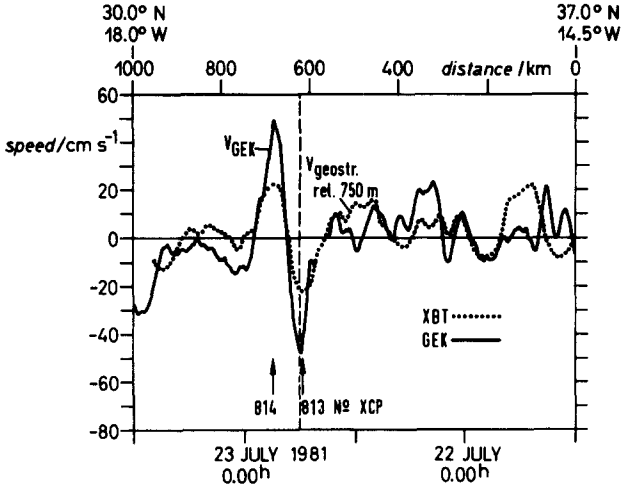

FIG. 5. Comparison of geostrophic surface velocities (derived from XBT using averaged *T/S* relationships) with hourly averaged G.E.K. velocities during *Meteor* 57, leg 3.

The geopotential anomalies inferred from temperature profiles are displayed together with the isotherms in Fig. 3(a). They have been converted to geostrophic velocities (Fig. 5) relative to 700 m depth. In addition to errors arising from the *T/S* relation, the derived velocities will not reveal any ageostrophic components, such as Ekman and inertial motions. This point is mentioned because in Fig. 5 the smoothed geostrophic velocities are compared with the hourly-averaged G.E.K. velocities. The agreement between the velocity measurements, where one finds the tight *T/S* relationship south of 34°N (at 480 km, Fig. 5), is good. A particularly convincing example is found in a strong current loop, or eddy, in the vicinity of Madeira (Fig. 5). Both series show similar flow reversals and magnitudes.

The vertical profile of the geopotential anomaly ΔD, derived from XBT's can be compared with velocity profiles obtained with the expendable current profiler. In the strongest feature near Madeira the two profiling methods yield practically identical results in the low vertical wavenumber range – as can be seen in Fig. 6.

Additional comparisons were made with all XCP/XBT combinations from leg 3. Because of several interruptions due to mooring work, we had to omit comparisons of the nonsynoptic XBT data sets from leg 4. In the case of leg 3 the XCP components from 7 drops were rotated parallel and normal to the ship's course. Since current profiles obtained by both methods contain an unknown offset, the resulting normal component of the XCP probes and the geostrophic profiles were fitted in the medium depth range 200–500 m to minimize relative differences. In Table 1 we show the rms difference between the two methods for the depth range 50–700 m.

Below the mixed layer we find an average scatter of O(2.5 cm s^{-1}). Our results indicate that the XBT's can successfully be used to calculate relative velocity profiles in a region of strong *T/S* correlation.

Another study undertaken with the present data is the determination of eddy covariances

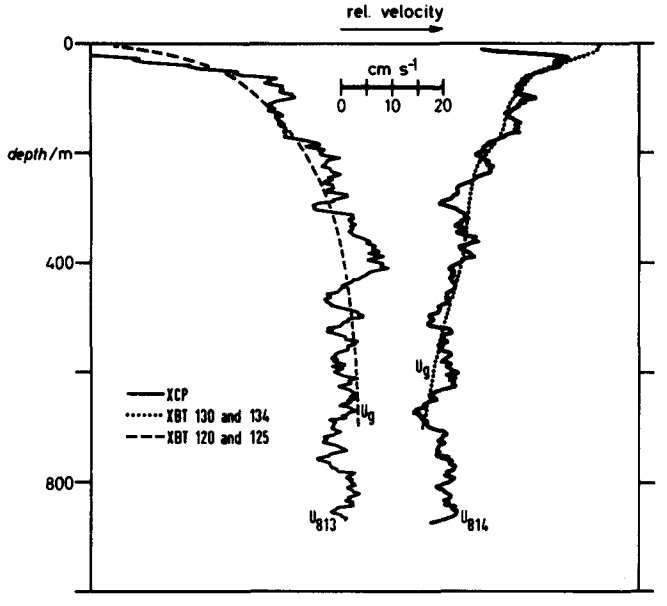

FIG. 6. Comparison of the XCP profiles 813 and 814 with geostrophic velocity profiles as derived from XBT pairs 130 and 134 and 120 and 125 using the averaged T/S relationship.

and transports. There are measurements or estimates of the eddy contribution in the subtropical gyre. VOORHIS, SCHROEDER and LEETMAA (1976) estimated eddy transports of temperature within mesoscale features in the MODE region. The only known direct observations are from moored current and temperature meters, which determine the temporal eddy covariances (BRYDEN, 1979). Another approach is to obtain velocity and temperature measurements in space and compute the spatial vT covariance. An eddy temperature flux will exist only if a significant correlation exists between v and T in either space or time.

In this section the focus will be on the large-scale or along-track observations from the G.E.K. and temperature measurements. Observations for the deep water leg from Cape Finisterre to the Canary Islands (leg 3) are shown in Fig. 7. Considerable variability is evident at horizontal wavelengths of 50–100 km. The temperature record contains a strong spatial trend. The single strong meander or eddy, already mentioned earlier, is present near the end of the section. Certain calculations were conducted with and without this feature to ensure that this one event did not dominate the statistics.

TABLE 1. DEPTH DEPENDENCE OF THE RMS DIFFERENCE BETWEEN XCP COMPONENTS PERPENDICULAR TO THE SHIP'S COURSE AND GEOSTROPHIC CURRENTS INFERRED FROM XBT OBSERVATIONS

depth (m)	50	100	150	200	250	300	400	500	600	700
$\pm \delta v$ (cm s^{-1})	2.1	1.4	1.9	1.8	2.5	2.6	2.2	3.9	4.1	6.7

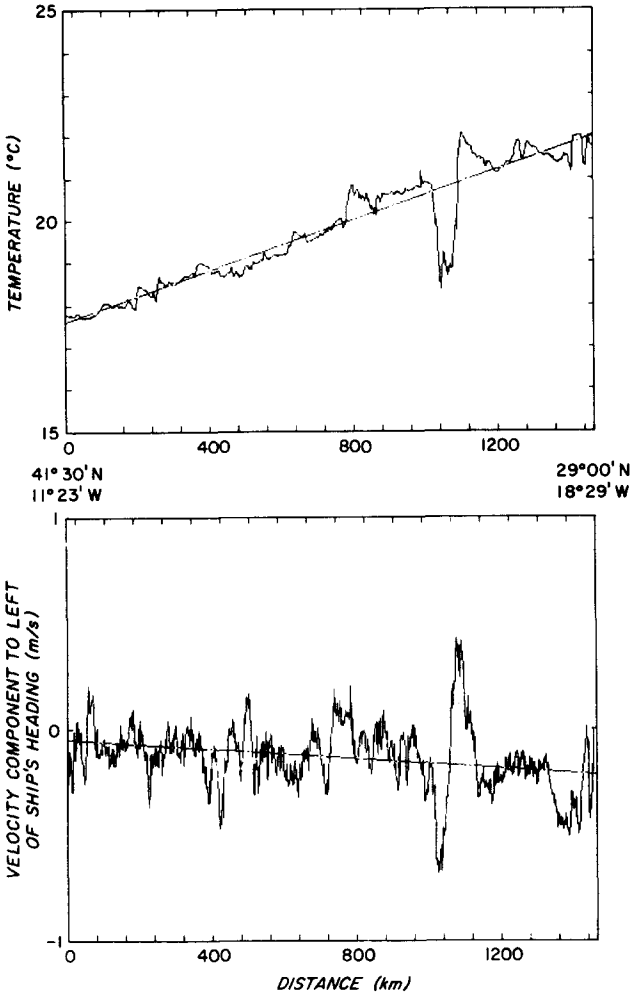

FIG. 7. G.E.K. velocity and temperature between Cape Finisterre and the Canary Islands. The dashed lines represent a linear least squares fit to the data. A strong spatial trend in the mean is clearly evident.

The lines superimposed on the speed and temperature data represent a linear least squares fit of the data against time. These linear fits were used to remove a spatial mean and trend from each of the four data subsets. The residues (v' and t') that remained are plotted in the lower two panels in Fig. 8.

In the upper panels of Fig. 8(a), the hourly average of the product of v' and t' is plotted below the spatial integral. Each data point is a 5-minute-averaged value of observations made every 30 s, and is assumed to represent a distance of 1.5 km. When one takes the product of the values on the top panel, and the water depth for which the G.E.K. values are representative, the eddy temperature flux for that depth can be specified. In the derivation of the eddy temperature fluxes we make use of the fact that, as will be deduced later from the finescale CTD survey, the depth interval south of 36°N for which the G.E.K. surface fluxes are representative is 200 m.

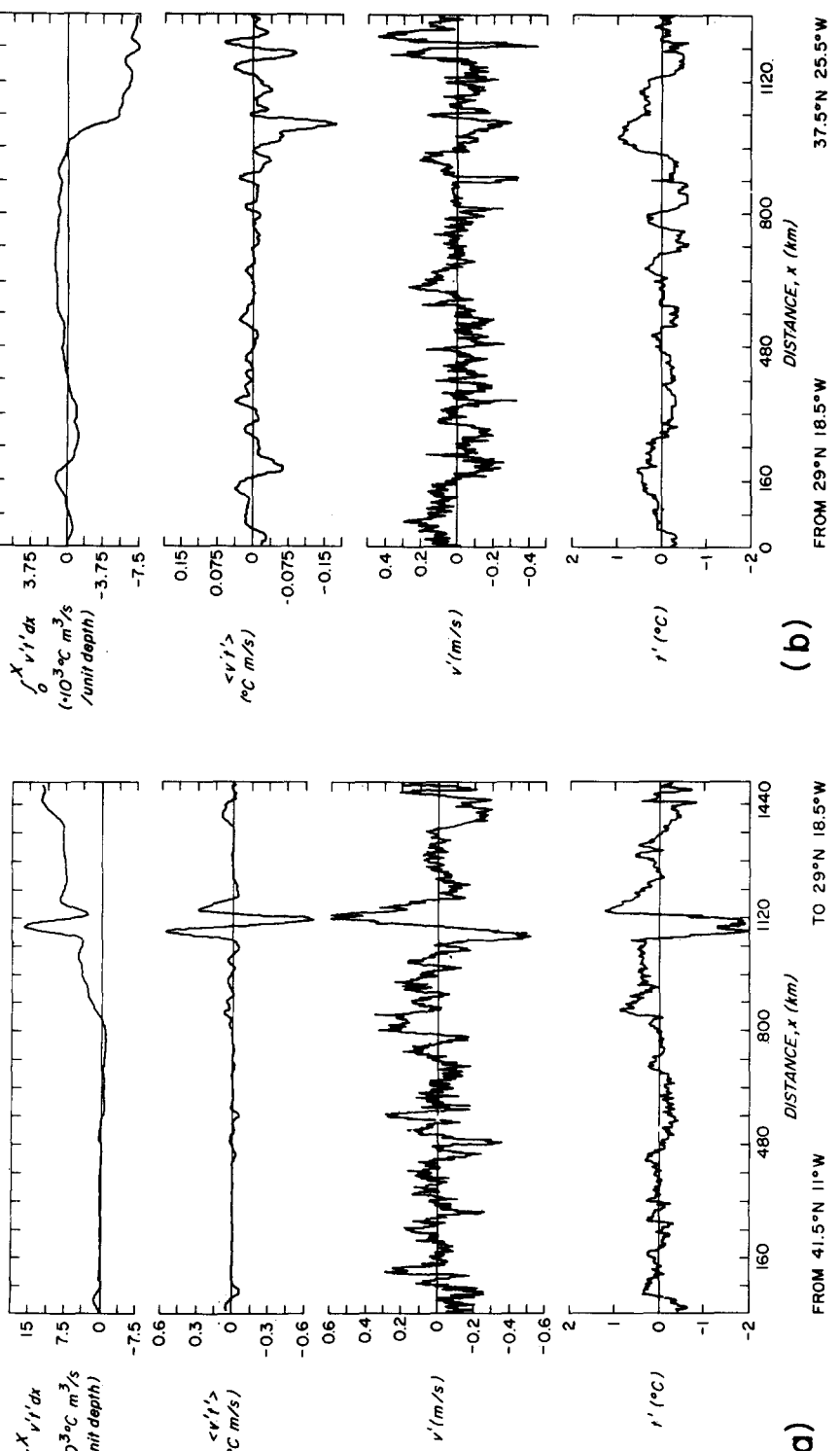

FIG. 8(a). G.E.K. and temperature measurements for the deep water leg from Cape Finisterre to the Canary Islands (adopted from SANFORD and SPAIN, 1982). In the upper panels the hourly average of the product of v' and t' is shown below the spatial integral along the track. Multiplication of the spatial integral value with the water depth for which the G.E.K. values are representative (200 m, see Section 4), specifies the eddy temperature transport. The residues v' and t' shown in the lower panels were obtained after removal of the linear spatial trend.

FIG. 8(b). G.E.K. and temperature measurements on leg 4 from Canary Islands to Azores [see Fig. 8(a)].

The eddy temperature transport along leg 3 is about 2.5×10^6 °C m^3 s^{-1} for a layer of 200 m depth; leg 4 has about 2/3 of that amount. The average value for legs 3 and 4 can be expressed as 1.4×10^3 °C m^3 s^{-1} km^{-1}. If we take into account that most of the variability along legs 3 and 4 occurred between 36°–30°N, this value may be augmented to 3.0×10^3 °C m^3 s^{-1} km^{-1}. VOORHIS, SCHROEDER and LEETMAA (1976) calculated an eddy temperature transport in the MODE region, centered near 28°N 70°W, of 10^4 °C m^3 s^{-1} km^{-1}. This calculation is probably an overestimate since the model assumed a rather large (2°C) temperature difference between northward and southward flows. The difference in energy levels between the eastern basin observations and the MODE area calculations is however not unexpected and results from the eddy kinetic energy differences between the eastern and western basins (WYRTKI *et al.*, 1976).

In a later discussion of the $v'T'$ distribution as inferred from the box shaped CTD survey, it will be emphasized that the eddy temperature flux is spatially patchy. The values reported here are the average for the total length of each leg.

In their discussion of the large scale structure of sea surface temperature, VOORHIS *et al.* (1976) concluded that surface currents associated with deep baroclinic mesoscale eddies were the primary agents for distorting the observed surface temperature field. Thus one might expect coherence between G.E.K. (i.e., baroclinic) velocities and surface temperature. As will be shown later when discussing mesoscale variability as observed during the finescale CTD survey, this mechanism seems to be applicable to the eastern basin and in fact would explain the observed high eddy temperature correlation.

Summarizing we find that little temperature and velocity correlation on leg 3 is observed until the 800 km point near Josephine Bank is reached [Fig. 8(a)]. South of this point the variables are more energetic and more correlated (cf. KNOLL, ZENK and BAUER, 1982). The integral $v'T'$ value beyond this point is 1.6×10^{-2} °C m s^{-1}. It is found that the surface perturbations extend well into the main thermocline [Fig. 3(b)].

Along leg 4 the $v'T'$ contributions are small and of variable sign until the 800 km point is reached. From this point until the Azores the observations reveal the same structure as seen on leg 3 800 km to the east. The averaged $v'T'$ value beyond this point is 2.1×10^{-2} °C m s^{-1}.

A qualitative idea of the depth dependence of the observed surface variability has been inferred through the combined use of XCP and XBT derived vertical velocity profiles. In the case of the cyclonic feature observed west of Madeira we were able to demonstrate that at least some of the observed enhanced variability between 36°N and 30°N had deeper velocity and temperature roots and was not confined only to the surface layer (Fig. 6). Thus on both legs we found a band of energetic structures between 36°N–30°N with a NW–SE alignment. From the CTD survey conducted later this feature turned out to be a continuous meandering flow band responsible for the enhanced variability and coincident with the Azores current as depicted by WÜST (1935) in Fig. 1.

4. AZORES CURRENT FRONTAL ZONE

4.1. *Main characteristics*

In order to develop a three dimensional quasisynoptic picture of the flow and property field in the region between Madeira and the Azores, *Poseidon* 86 conducted an upper ocean (1,500 m) CTD survey. The continuity and the spatial alignment of the band of enhanced energetic structures, observed earlier during the *Meteor* 57 underway measurements, was investigated [Fig. 2(b)].

The historical data base indicates a weak, broad eastward flow in this area (LEETMAA, NIILER and STOMMEL, 1977; SIEDLER and STRAMMA, 1983). Our observations, presented as objectively-mapped mixed layer temperature, salinity and dynamic topography fields in Fig. 9, reveal a strong, narrow eastward flow with much meandering. The flow has a maximum of about 25 cm s^{-1}, a width of 60 km, an e-folding depth of 600 m and a volume transport of about $10^7 m^3 s^{-1}$. KÄSE and SIEDLER (1982) argue that the jet, or front, is an integral part of the North Atlantic gyre circulation. That is, this flow, which we call the Azores Current (DIETRICH, KALLE, KRAUSS and SIEDLER, 1975), originates at the point where the Gulf Stream separates into this branch and the North Atlantic Branch at about 40°N 45°W (KRAUSS and MEINCKE, 1982; GOULD, 1984). Clearly, the meandering of this flow broadens the property gradients and makes the flow appear to be a broad one consistent with the picture based on historical data (EMERY, 1983).

The geopotential topography chart shown in Fig. 9(c) reveals that three, separate horizontal scales are present in the region. First, there is the box-wide scale that is related to the mean or gyre circulation. Second, there is a smaller scale associated with a meandering flow, possibly Rossby waves originating at the eastern boundary of the Canary Basin. Third, there is the mesoscale eddy field.

Across the meridional extent of the box there existed a difference of 1.7 $m^2 s^{-2}$ in the geopotential anomaly field. A linear multiple regression was made on the field of geopotential topography to determine the box-wide mean flow. Planes were fitted to more than five depth levels. About 50–60% of the total variance is contributed by the linear trend to the geopotential topography depending on the depth level. The flow has a tendency to turn with depth in the counterclockwise sense (13° between 150 and 400 m; cf. Table 2). The volume transport through the box was about $13 \times 10^6 m^3 s^{-1}$ at a direction principally to the east with only a slight northward bias. This result is in contradiction with the classic Sverdrup flow in this region which is understood to be southward. The 1.7 $m^2 s^{-2}$ difference represents about 40% of the total baroclinic recirculation in the eastern part of the subtropical gyre (STOMMEL, NIILER and ANATI, 1978).

It is interesting to note that OLBERS, WILLEBRAND and WENZEL (1982) resolve a current branch in their calculation of absolute velocities using the local β-spiral methods. The current band is connected with the Gulf Stream and is bounded at 150 m depth by the 16°C isotherm on the northern side and by the 18°C isotherm on the south. This temperature structure is identical to that found in the present investigation. At first it may seem strange that observations in one season compare favorably with yearly-averaged observations. Wintertime convection mixes the water column in this area to a depth of 150–200 m. Thus the springtime temperature at 150 m is typical of the long-term mean because of the vigorous mixing. In the summer there is much of this 16°–18°C water in the seasonal thermocline. This water has a low vertical gradient, similar to the so-called 18-degree-water of the Sargasso Sea, and more formally known as Subtropical Mode Water (WARREN, 1972; MCCARTNEY, 1982). Recall the XBT sections of Fig. 3 where this water mass is labeled by the shaded area. It was confined to and south of the Azores Current. The 2°C-temperature step across the current is also found in the summertime section from *Meteor* 57 at the surface, but at absolute temperatures that are 4°C higher than at 150 m.

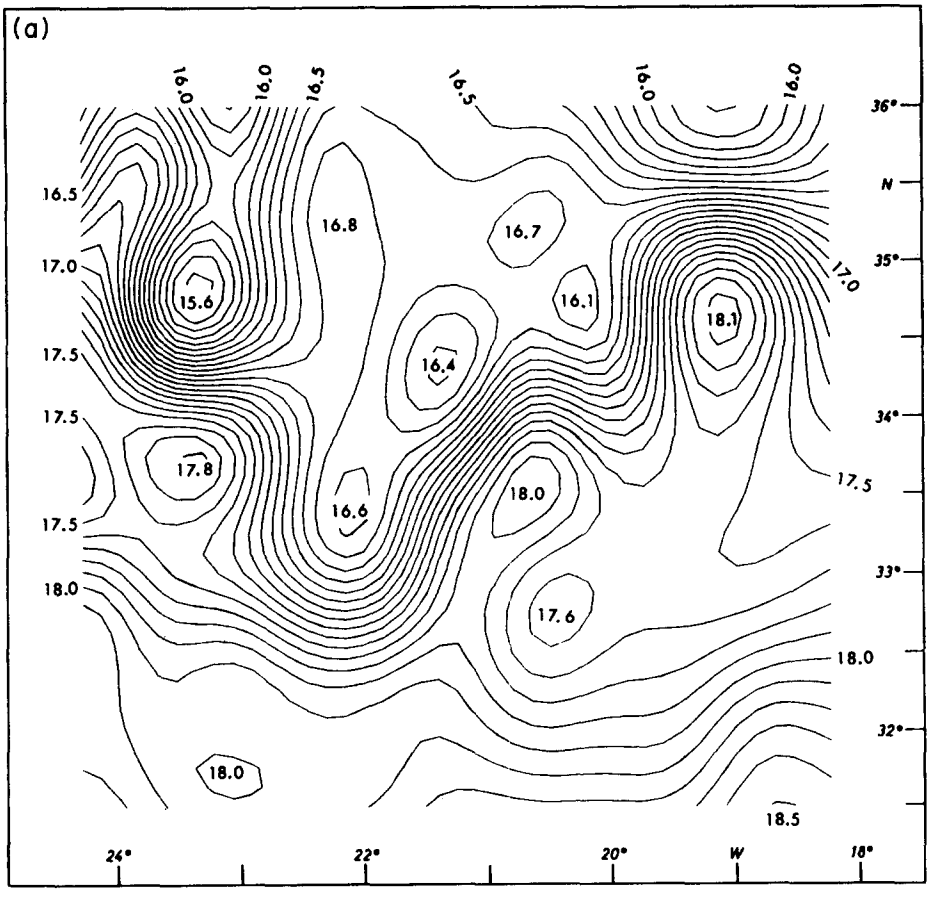

FIG. 9. Objective analysis of 25 m mixed layer temperature (a), salinity (b) and dynamic topography (c) relative to 1500 dbar. The approximate centre of the frontal band is marked in (c) by the 13.5 $m^2 s^{-2}$ isoline. Station pattern of *Poseidon* 86 CTD survey see Fig. 2(b).

4.2. *Meander-scale variability*

In the center of the survey region is a large cyclonic anomaly in the geopotential field. This energetic feature dominates much of the flow and property distribution and must be removed to reveal the underlying, smaller-scale variability. After subtraction of the spatial linear trend a simple Rossby wave model:

$$\psi(x) = P \sin(\eta y - \phi_1) \cos(\kappa x - \phi_2),$$

was fitted to the residual geopotential anomaly field at different depth levels. The composite mean field, i.e. linear trend plus Rossby wave field at 25 m depth is displayed in Fig. 10. Removal of the wave field reduces the meander-scale structure almost completely and reveals a mesoscale eddy field (Fig. 11). These fits and the trajectories of numerous driftbuoys (Fig. 12) indicate that the horizontal wavelength of this feature (570 km) is about the size of the box. Because the Mid-Atlantic Ridge and the coast of Africa act as lateral boundaries, a set of discrete, standing Rossby waves is possible. For any wave having a wavelength considerably larger than the Rossby radius of deformation for the first vertical mode R_1, the frequency is given by

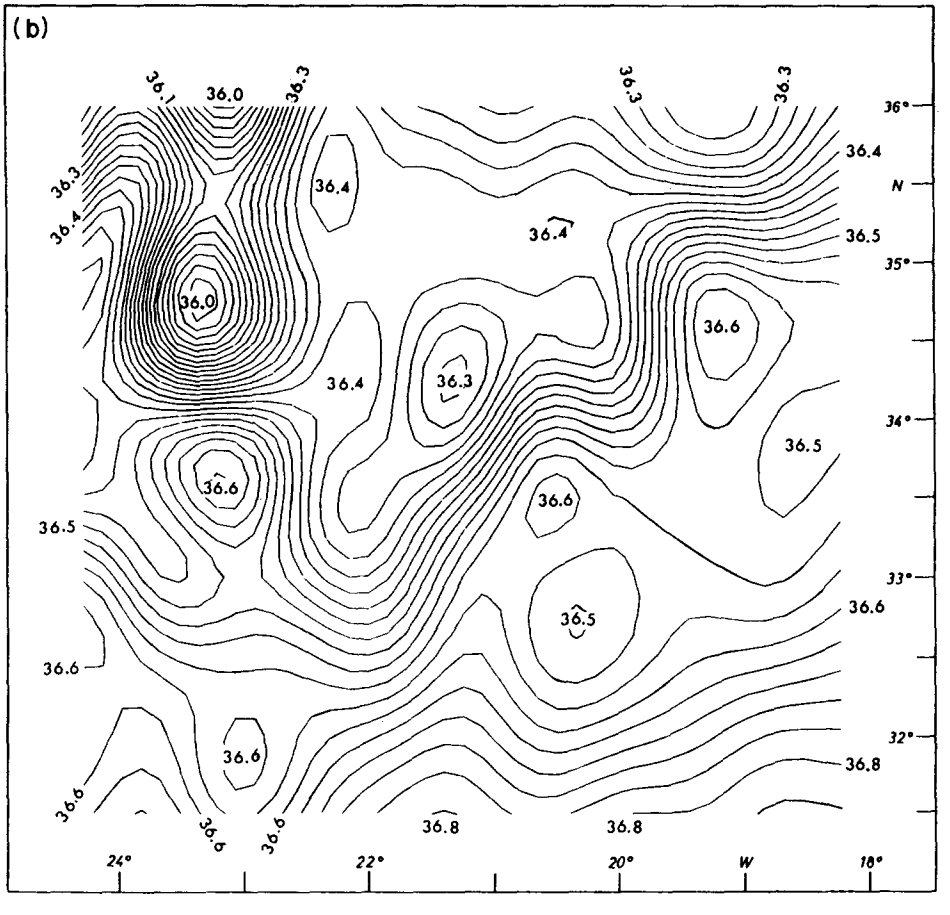

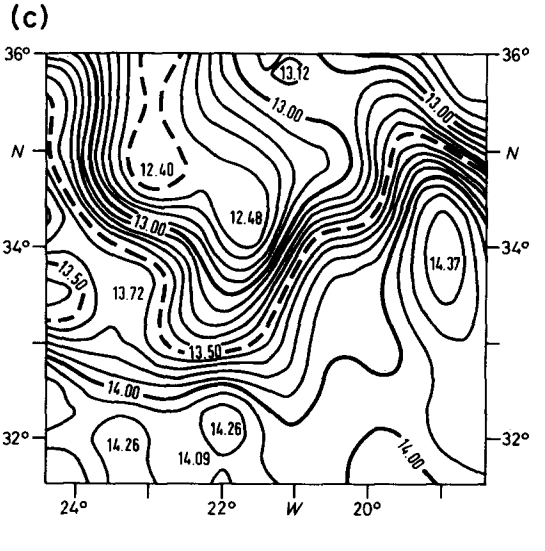

FIG. 9. (*Continued*)

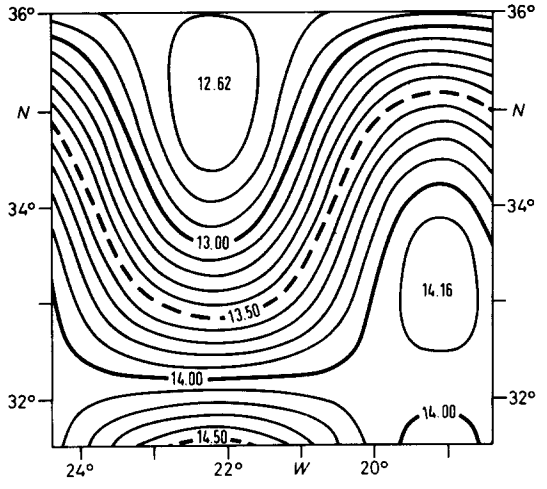

FIG. 10. Superposition of linear trend and Rossby wave fit for geopotential topography ($m^2 s^{-2}$) at 25 dbar relative to 1500 dbar. Further superposition of the anomaly field displayed in Fig. 11 yields the total geopotential field shown in Fig. 9(c).

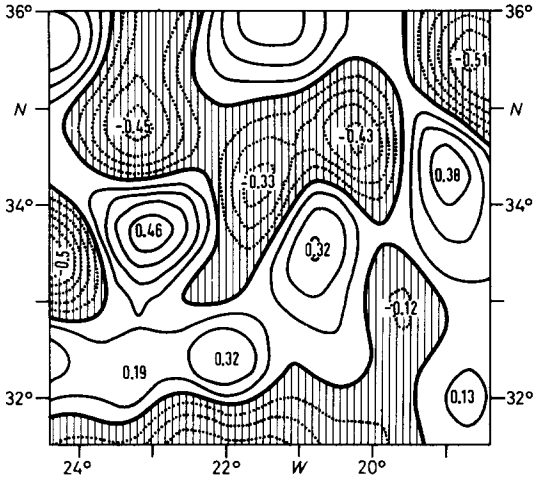

FIG. 11. Objective analysis of the geopoential anomaly field ($m^2 s^{-2}$) at 25 dbar relative to 1500 dbar after subtraction of the linear spatial trend and removal of the Rossby wave field. Note that the dominant scale is about 100 km.

$\omega = \beta R_1/2$. The phase velocity of the hypothetical Rossby wave is given as $c = \beta R_1^2$, which yields a horizontal wavelength of $4\pi R_1$. The first mode Rossby radius of deformation is about 45 km, so that the wavelength is about 600 km, a scale that is consistent with the fit made earlier to the observations. The period corresponding to this wave is 160 days. Variability at this time scale is evident in the moored current meter records. Fig. 13(a) presents the 640-day record of current at 700 m at the central mooring position. Because the spectrum has a low-frequency plateau and a higher-frequency dependence of ω^{-2} the time series of both velocity components were fitted to a second order, auto-regressive process.

The period of the estimated autocorrelation function for the north component is 138 days

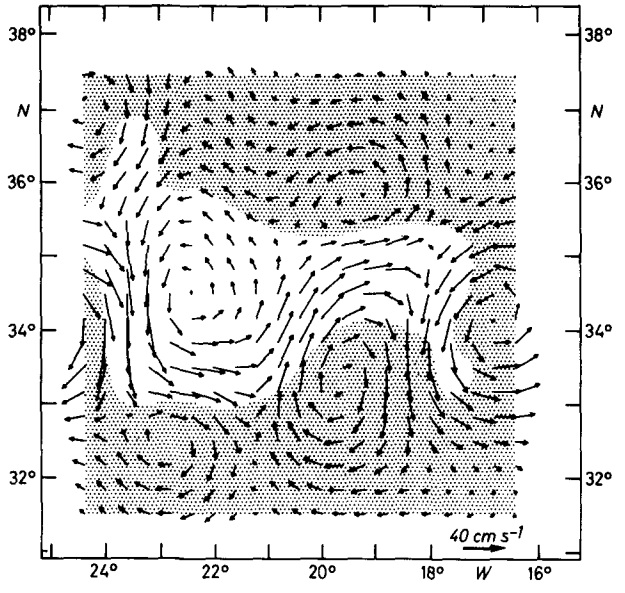

FIG. 12. Objective analysis of driftbuoy trajectories observed in the area between Madeira and the Azores between 1982 year days 70–100. The drifters were drogued at a depth of 100 m. In the dotted area the estimated error variance exceeds 50% of the variance of the true velocity field. Due to the sparse spatial resolution of the quasi-Eulerian input velocity field derived from the Lagrangian trajectories, all eddy variability on scales smaller than 100 km has been treated as noise and essentially been smoothed out.

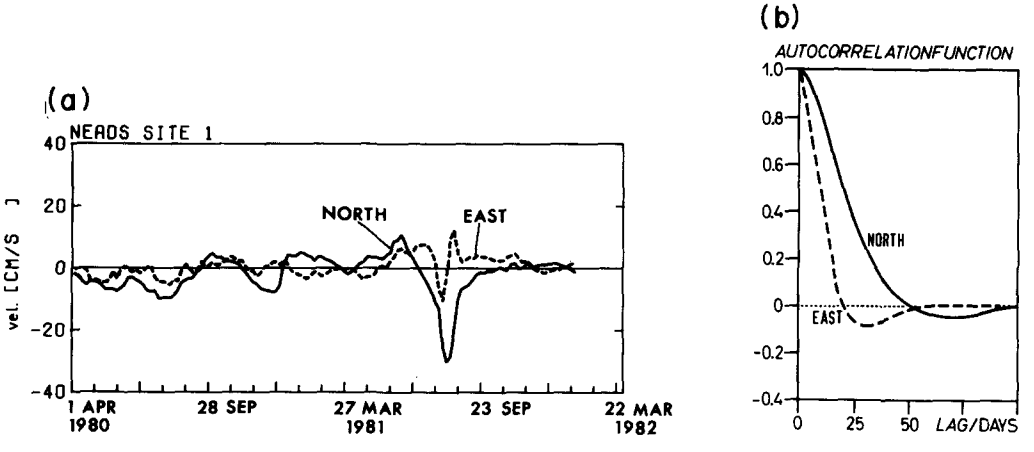

FIG. 13(a). Moored current meter record of the central mooring position (33°N 22°W) at 700 m depth (courtesy of T. J. MÜLLER).

FIG. 13(b). Model autocorrelation function of the velocity components obtained by fitting a second order autoregressive process to the time-series displayed in Fig. 13(a).

[Fig. 13(b)], whereas that for the east component is 60 days. This indicates that distinct processes determine the zonal and meridional components. Westward propagating Rossby waves have the most variability in the meridional component. The observed dominant period of 138 days compares favorably with the theoretical period appropriate to the observed horizontal

scale of motion. On the other hand, the 60-day period is consistent with that found by other investigations of mesoscale eddies (WUNSCH, 1981).

4.3. *Mesoscale variability*

Focusing now on the mesoscale variability, we examine the residue from the Rossby wave fit after subtraction of the linear field. An objective analysis has been made of the residual fields of temperature and topography of the geopotential anomaly. The horizontal covariance function used in this analysis was derived from the CTD data set and the G.E.K. velocity observations. HILLER and KÄSE (1983) determined the model covariance functions from a non-linear parameter fit to the raw covariances. An isotropic, Gaussian function with standard width, L, of 60 km was chosen as the most suitable one. This model was then compared with the G.E.K. correlations, which are by the nature of the measurements transverse correlations. For the streamfunction model covariance function $F(r)$ derived from the CTD data, the corresponding transverse velocity correlation is

$$G(r) = -\frac{\partial^2 F(r)}{\partial r^2}$$

(BRETHERTON, DAVIS and FANDRY, 1976), and has a zero crossing at 60 km. This scale is about that found in the G.E.K. data.

The near-surface (25 m) topography of the geopotential anomaly from objective analysis is presented in Fig. 9(c). Except near the boundaries the uncertainty in the mapping of geopotential topography is 0.1 $m^2 s^{-2}$. The features after removal of the large scale mean flow are somewhat elongated and of less elevation than similar disturbances found in the western North Atlantic during MODE (MODE GROUP, 1978) and POLYMODE (MCWILLIAMS *et al.*, 1983). The field has an rms amplitude of 0.55 $m^2 s^{-2}$. It is important to note that although the geopotential topography field is less energetic in the eastern basin, the length scales are shorter and the resulting velocities larger. The close approach of high and low disturbances may lead to enhanced frontogenesis as has been suggested by VOORHIS, SCHROEDER and LEETMAA (1976).

It is interesting to note that small-scale variability in the G.E.K. velocities and in the thermosalinograph recordings increased considerably when *Meteor*, during legs 3 and 4, entered regions of sharp temperature and salinity gradients. An example was presented in Fig. 3 (near XCP No. 813/14). The temperature and salinity steps across the feature are about 2°C and 0.3, the same differences that are observed across the meander found in the *Poseidon* CTD survey (Fig. 9). This suggests that a continuous frontal zone exists as a northern boundary of the central subtropical gyre. This is confirmed by the satellite buoys which drift eastward in a meandering pattern until they reach Madeira (Fig. 12) and is substantiated by measurements of GOULD (1984) and POLLARD and PU (1984).

The observations of temperature and velocity correlations from the towed data of *Meteor* 57 encouraged us to make similar calculations with the CTD data from *Poseidon* 86. One of the evident aspects of the towed observations is the spatial intermittency of the eddy heat transport. The coverage of the *Poseidon* density survey provided the opportunity to investigate this intermittency and to isolate the region of largest flux. We use the CTD data to determine the composite mean field, i.e. the spatial linear trend plus Rossby wave field for geopotential topography and temperature at different depth levels. Removal of this mean field yields the anomaly fields for temperature and geostrophic velocity. An optimal estimation

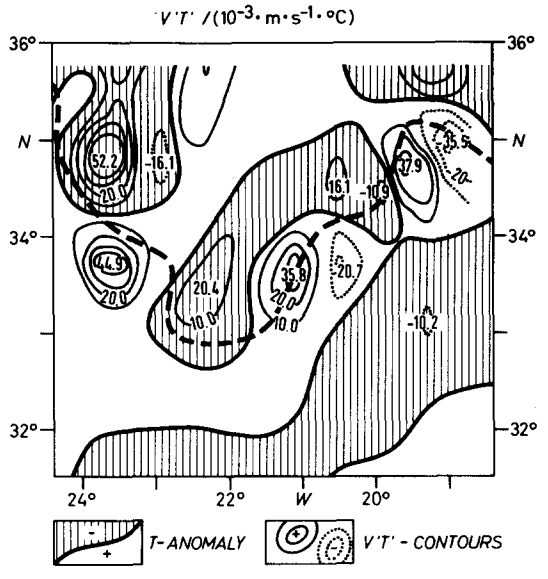

FIG. 14. Distribution of $v'T'$ at 25 dbar. (Contours of noisy features of magnitude smaller than 10×10^{-3} °C m s^{-1} have been suppressed.) Note that on the western side the major positive $v'T'$ contributions coincide with negative temperature anomalies, whereas on the eastern side the major postive $v'T'$ contributions occur together with positive temperature anomalies indicating advection of cold water southward and recirculation of warm water northward by mesoscale eddies along the frontal band [dashed line according to Fig. 9(c) marks the approximate center of the frontal zone]. Due to the phase shift between velocity and temperature fields the resulting scales of $v'T'$ are smaller than the scale of the residual eddy field shown in Fig. 11.

technique (BRETHERTON, DAVIS and FANDRY 1976) is used to obtain $v'T'$ products on a uniform grid in the observational area (Fig. 14).

The calculations show that there is eddy temperature transport and it is of the same sign and magnitude as observed in the towed measurements from *Meteor* 57. In the mixed layer and upper thermocline the distribution of $v'T'$ was derived at the 25, 150, 250 and 400 m depth levels.

The distribution of $v'T'$ is shown in Fig. 14 at 25 m depth. The major $v'T'$ contributions occur on the periphery of the cold pool or dynamic low of Fig. 9(c). The process appears to be the same as that suggested by VOORHIS, SCHROEDER and LEETMAA (1976), namely, that cold water is advected southward and warm water is recirculated northward by the mesoscale eddies as they exchange water and properties with the frontal band flow. The pattern at each of the four levels in the upper 500 m layer is similar with respect to latitude in that the flux in the tranquil region south of 33°N is negligible and to the north it becomes measurable. One of the most interesting aspects of these determinations is the vertical integral of eddy covariance. The results of vertical averaging of the horizontal $v'T'$ distributions in the upper 500 m layer is displayed in Fig. 15, where zonal averaging has been used in order to derive the latitudinal dependence of $\langle v'T' \rangle$. Since we are mainly concerned with the investigation of meriodional eddy heat transport across the frontal band, zonal averaging is used to obtain estimates of eddy temperature covariances $\langle v'T' \rangle$.

The $u'T'$ distributions in the upper 500 m level have been derived as well. Again, significant values of $u'T'$ are found only along the frontal band, but with a smaller magnitude than the

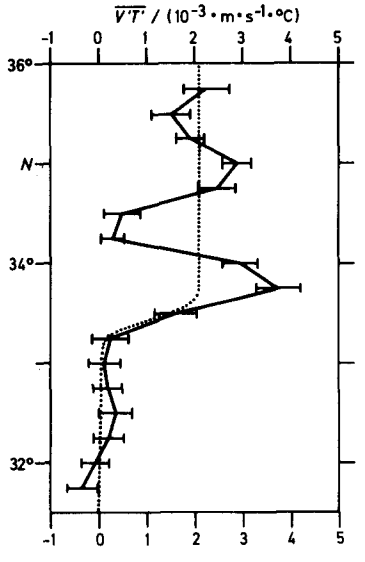

FIG. 15. Zonal averages of

$$\overline{v'T'} = \frac{1}{L}\int_0^{500} v'T'\,dz$$

representing the meridional dependence of the total $\overline{v'T'}$ estimate in the upper 500 m layer. A fitted tanh-model demonstrates the different levels of eddy covariance north and south of the frontal band. The error bars are standard errors which have been derived from the error maps of the geopotential anomaly and temperature fields as predicted by objective analysis. They are not significance levels of mean values in the common statistical sense.

corresponding $v'T'$ values. This is reflected in the different correlation coefficients for the total box area. At the 25 m level the correlation of $v'T'$ is 0.34 whereas the correlation of $u'T'$ is only about 0.09. This means that the observed eddy heat transport across the front is basically directed northward with negligible zonal components. The towed observations were unable to determine the depth interval over which the surface eddy covariances were representative. According to Fig. 15 the surface covariances are typical over hundreds of meters. A typical depth scale can be defined by the relation:

$$Z = \frac{\int \langle v'T' \rangle\,dz}{\langle v'T' \rangle_{25}},$$

where v' and T' are the residual fields after the removal of the spatial mean fields as defined by the Rossby wave fit and linear trend. For the integration the depth interval between the surface and 500 m, a depth sufficiently above the anomalous Mediterranean water, was chosen. The average value of Z in the box north of 33°N is 200 m. The box averaged meridional eddy temperature transport north of 33°N is $(0.95 \pm 0.14) \times 10^3\,°C\,m^3\,s^{-1}\,km^{-1}$ with a zonal component of $(0.28 \pm 0.4) \times 10^3\,°C\,m^3\,s^{-1}\,km^{-1}$. Obviously we cannot distinguish the zonal component significantly from zero. The calculated 95% significance levels have been based on the estimated degrees of freedom during the experiment.

Because of the short spatial correlation scale of 60 km, each station during the *Poseidon* 86 CTD survey can be regarded as an independent observation. On this basis the CTD analysis has about 80 degrees of freedom, of which 45 have been attributed to the area north of 33°N.

For the overall $v'T'$ correlation coefficient this results in a zero correlation level of 0.22. At the 25 m and 400 m levels with $v'T'$ correlations of 0.34 and 0.24, respectively, we therefore have significant correlations. At the 150 m and 250 m levels, which are influenced by internal waves at the base of the deep surface mixed layer, the values of 0.16 and 0.14 do not surpass the zero correlation level, due to the amplified variance of the temperature fluctuations.

In the case of *Meteor* 57, the degrees of freedom are about half that of the CTD survey, or about 40. The 95% significance level is therefore 0.31, and the observed correlation coefficient is only about 0.15. The lower correlation is in part due to the larger bandwidth of the towed measurements and the majority of the data coming from the tranquil region, rather than from the much more active frontal region. If we confine these calculations to the regions of enhanced variability during legs 3 and 4 of *Meteor* 57, we obtain correlation coefficients of 0.23 and 0.38 respectively. These values compare well with the CTD survey surface $v'T'$ correlation. However, due to the reduced number of degrees of freedom, they lie below the corresponding zero significance levels.

5. LOCAL TEMPERATURE BALANCE

Our observations were concerned with upper ocean mean flows and eddy heat transports in the region between Madeira and the Azores. The mean field consists of an eastward flow in the upper 700 m which, presumably, is the Azores Current, an eastern basin extension of the Gulf Stream. This current is the northern boundary of a region that is notably quiescent in terms of eddy and mean flows west of Madeira and that extends beyond the study region to the south [cf. Fig. 8(b); see also DANTZLER, 1977; EMERY, 1983]. The Azores Current carries significant heat into the region and may be the source for much of the eddy variability.

There are few comparable observations of significant $v'T'$ correlations in the open ocean. BRYDEN (1979) and JOYCE, ZENK and TOOLE (1978) report values for eddy covariances in the Drake Passage, but otherwise the eddy contributions are only inferred from the divergence of the mean advection terms (MCWILLIAMS, 1983).

On the basis of the observations we can estimate at least two of the terms in the temperature transport balance. The balance is formulated in terms of the spatial mean and perturbation contributions. In the absence of local sources and sinks for temperature the mean advection must be balanced by the eddy flux divergence. Neglecting molecular conduction and temporal changes, the balance equation is:

$$\bar{\mathbf{u}}_H \cdot \nabla_H \bar{T} + \bar{w} \frac{\overline{\partial T}}{\partial z} + \nabla_H \cdot \overline{\mathbf{u}'T'} + \frac{\partial \overline{w'T'}}{\partial z} = 0. \tag{1}$$

Note that in the process of estimating the different components of the balance equation we were forced to replace ensemble averages by zonal averages in order to estimate the expected value of the different terms. Because of our separation of the mean temperature and geopotential topography fields into linear spatial trend, and Rossby wave we have to consider two components of the horizontal advection term. Due to the in-phase vertical coherence there is no contribution to the horizontal advection term by the Rossby wave. Further, there is no measurable correlation between the Rossby wave and the mesoscale eddy field, and consequently no cross terms appear in the balance equation.

In Table 2 the horizontal advection terms as derived from the linear multiple regression of the temperature and geopotential anomaly fields are shown. Vertical averaging of the advection terms in the upper 500 m layer leads to a mean horizontal advection of $(-2.3 \pm 0.8) \times 10^{-8}\,^{\circ}\mathrm{C\,s^{-1}}$.

TABLE 2. RESULTS OF THE LINEAR MULTIPLE REGRESSION OF TEMPERATURE AND GEOPOTENTIAL ANOMALY FIELDS. ALL SIGNIFICANCE LEVELS ARE 67% STANDARD ERRORS

Depth z (m)	Mean circulation $\bar{u}$ (cm s^{-1})	Mean circulation $\bar{v}$ (cm s^{-1})	Horizontal temperature gradients $\frac{\partial \bar{T}}{\partial x}$ (10^{-6} °C m^{-1})	Horizontal temperature gradients $\frac{\partial \bar{T}}{\partial y}$ (10^{-6} °C m^{-1})	Horizontal advection term $\bar{\mathbf{u}}_H \cdot \nabla_H \bar{T}$ (10^{-8} °C s^{-1})
25	3.8 ± 0.40	0.68 ± 0.39	0.50 ± 0.28	−3.9 ± 0.30	−0.74 ± 1.86
150	3.2 ± 0.37	0.76 ± 0.36	0.63 ± 0.54	−6.2 ± 0.60	−2.7 ± 2.85
250	2.6 ± 0.30	0.73 ± 0.30	0.35 ± 0.46	−5.5 ± 0.50	−3.1 ± 2.07
400	1.8 ± 0.25	0.76 ± 0.24	−0.07 ± 0.27	−3.1 ± 0.30	−2.5 ± 0.91

Another possibility to calculate the mean advection term in eq. (1) is to determine the rotation of current with depth. With the aid of the thermal wind equation one gets according to BRYDEN (1976):

$$\mathbf{u}_H \cdot \nabla_H T = \frac{f}{g\alpha}\left(v\frac{\partial u}{\partial z} - u\frac{\partial v}{\partial z}\right) = \frac{f}{g\alpha}\left(S^2\frac{\partial \phi}{\partial z}\right), \tag{2}$$

where ϕ is the direction of current as a function of depth and

$$\alpha = -\frac{\partial \rho}{\partial T}, \qquad S^2 = u^2 + v^2.$$

The value calculated by relation (2) amounts to $(-3.4 \pm 1.8) \times 10^{-8}$ °C s^{-1}. The mean horizontal advection term as derived directly from the inclination of the planes fitted to the temperature and geopotential anomaly fields by multiple regression, which takes account of the actual density variation with depth, is thus smaller, but within the significance levels consistent with the Bryden estimate. It should be noted that differences can only arise through deviations from a linear T/S relationship.

An estimate of the mean vertical velocity term could be inferred through the linear Sverdrup relation:

$$\bar{W} = W_{\text{Ekman}} - \frac{\beta}{f}\int_0^z v(z')\,dz'. \tag{3}$$

Since our observational area lies in the subtropical convergence zone, downwelling is expected to occur. This is confirmed by the maps of LEETMA and BUNKER (1978) where the Ekman velocity is downward in this region and amounts to about 10^{-6} m s^{-1}. The integral of (3) between the surface and 500 m is 0.9×10^{-6} m s^{-1}. The mean vertical gradient of temperature is about 10^{-2} °C m^{-1} averaged between 200 (the bottom of the surface mixed layer) and 700 m. The total estimate for the mean vertical velocity term is -1.9×10^{-8} °C s^{-1}. Both of the above flux terms represent warming of the region. However, this estimate of the mean vertical velocity term may be erroneous for several reasons. First we do not have adequate information about the actual Ekman pumping at the time of the *Poseidon* CTD survey. Second, a reexamination of the IGY section at 36°N in 1981 (D. ROEMMICH, *pers. commun.*) revealed a significant deviation of the observed meridional transport from the theoretical Sverdrup transport.

The remaining terms of (1) represent the eddy flux divergence. The *Poseidon* CTD observations show that the $u'T'$ contribution is negligible and the divergence is mainly due to the

$v'T'$ contribution. An estimate for this term is available from Fig. 15. The difference in the mean values of $\overline{v'T'}$ in the northern active and southern tranquil region amounts to $(2.1 \pm 0.3) \times 10^{-3}\,^{\circ}\mathrm{C\,m\,s^{-1}}$ over the distance of the frontal scale of about 100 km. The resulting contribution of the eddy flux divergence term is $2.1 \times 10^{-8}\,^{\circ}\mathrm{C\,s^{-1}}$ and corresponds to cooling of the region. The final term is not directly measured and must be inferred from a model.

Since the residual of the contributions ($-2.1 \times 10^{-8}\,^{\circ}\mathrm{C\,s^{-1}}$) is mainly due to the warming by vertical advection which is largely uncertain, we find that the basic balance is between the horizontal advection and eddy flux divergence. Whether there is additional warming through vertical advection or a vertical flux divergence cannot be deduced from our observations.

In addition, all terms may suffer from local changes during the quasisynoptic CTD survey; especially with the present data set the question is left open as to how much the local rate of temperature change contributes to the heat balance.

All estimated terms were based on an integral over the upper 500 m. Closer examination of the mixed layer alone suggests a different balance. Since there is no significant geostrophic shear in the mixed layer, the horizontal advection term vanishes (cf. Table 2). On the other hand the meridional flux divergence is strongest in the mixed layer ($4.8 \times 10^{-8}\,^{\circ}\mathrm{C\,s^{-1}}$) and corresponds to a cooling of the mixed layer in the frontal domain of 0.13°C in one month. This could either represent a seasonal local rate of temperature change or be balanced by a net heat surface influx of $20\,\mathrm{W\,m^{-2}}$. Finally it should be pointed out, that the eddy flux divergence has a maximum value in a 100 km central region, whereas the horizontal advection occurs throughout the entire survey region.

6. DISCUSSION

The present study is at the northern boundary of the inner subtropical gyre. In the center of the gyre the expected balance is one in which eddy processes are ignored (DICKSON, 1983), and the primary balance is between the mean advection terms of (1), resulting in a clockwise turning of the mean velocity vector with depth and downwelling. For example, ARMI and STOMMEL (1983) report observations of the clockwise turning of current with depth in the upper 800–1,000 m. On the other hand, the current rotates counterclockwise with depth in our study. We find, however, that the vertical motion is downward, as is typical of the mid gyre. The apparent contradiction is resolved by noting that we find significant eddy contributions, ones not considered or thought to be important in the mid-gyre experiments. It is interesting to note that KEFFER and NIILER (1982) also report significant eddy flux divergences and deviations from the predicted Sverdrup transport in the western part of the North Atlantic.

That the meridional temperature flux exists solely within and to the north of the meander and not to the south is consistent with the predictions of baroclinic instability. It is well known that baroclinic instability produces lateral temperature fluxes, and that the eddy temperature fluxes are proportional to the mean temperature gradient squared (PEDLOSKY, 1979). It thus seems likely that the lack of a significant temperature flux results from the absence of a strong mean meridional temperature gradient to the south of the meandering jet-like Azores Current. It should be noted, however, that in the present case it is not clear that classical theory applies due to the fact that the scales between the current jet and the resulting eddies differ less than one order of magnitude. We, therefore, choose not to investigate whether or not the necessary conditions for instability have been met.

Since the divergence of the heat flux of the fluctuations $(\partial/\partial y)(\overline{v'T'})$ is positive, this will

lead to a decrease in the available potential energy of the zonally averaged flow and consequently increase the energy of the fluctuations. Conversion of mean available potential energy to eddy energy in the absence of friction and horizontal shear of the mean flow is given (PEDLOSKY, 1979) by:

$$S = -\frac{\rho_0 g\alpha \overline{v'T'}\,\partial\bar{T}/\partial y}{|\partial\bar{T}/\partial z|}$$

which for

$$\partial\bar{T}/\partial y = -2\times10^{-5}\,^{\circ}\mathrm{C\,m^{-1}} \text{ (cross frontal gradient)};$$

$$\alpha = 10^{-4}\,^{\circ}\mathrm{C^{-1}},$$

$$\overline{v'T'} = 2\times10^{-3}\,^{\circ}\mathrm{C\,m\,s^{-1}};$$

$$|\partial\bar{T}/\partial z| = 10^{-2}\,^{\circ}\mathrm{C\,m\,s^{-1}};$$

yields $4\times10^{-6}\,\mathrm{J\,m^{-3}s^{-1}}$.

BRYDEN (1979) found a conversion rate of $1.2\times10^{-5}\,\mathrm{J\,m^{-3}s^{-1}}$ in the Antarctic Polar Front, while WILLEBRAND and MEINCKE (1980) report a value of $1.5\times10^{-4}\,\mathrm{J\,m^{-3}\,s^{-1}}$ in the Iceland–Scotland frontal zone.

The average eddy kinetic energy $\rho_0(\overline{u'^2}+\overline{v'^2})/2$ is estimated to be $1.5\,\mathrm{J\,m^{-3}}$ and the potential energy of the perturbations to be $g\alpha\overline{T}'^2/2|\partial T/\partial z|$ is $5\,\mathrm{J\,m^{-3}}$. Dividing the sum of the kinetic and potential energy by the conversion rate of $4\times10^{-6}\,\mathrm{J\,m^{-3}s^{-1}}$, we obtain a time scale of 19 days for the fluctuations to grow from zero to their average energy level.

By comparing their conversion rate with an estimate of the local input rate due to wind forcing, WILLEBRAND and MEINCKE (1980) argue that baroclinic stability is a more efficient process. With a typical wind stress and a velocity amplitude for our experimental site, $\tau_{\mathrm{rms}} = 0.1\,\mathrm{N\,m^{-2}}$ and $U_{\mathrm{rms}} = 0.05\,\mathrm{m\,s^{-1}}$, we estimate that the input rate due to wind forcing is smaller than $3\times10^{-6}\,\mathrm{J\,m^{-3}s^{-1}}$, assuming a correlation coefficient $C_{\tau u} \leqslant 0.3$. Thus, the conversion of mean potential energy is at least as effective as the local direct atmospheric generation.

A major heat source is the eastward moving, relatively narrow Azores Current. This current carries about $10^7\,\mathrm{m^3s^{-1}}$ relative to 1500 m and is characterized by extensive meandering. The eddy heat flux observed along the front is directed northward with $\overline{v'T'} = 4.8\times10^{-3}\,^{\circ}\mathrm{C\,m\,s^{-1}}$, a value which is significantly different from zero and representative for a 200 m vertical integral scale. The corresponding eddy heat flux is $2.0\times10^4\,\mathrm{W\,m^{-2}}$. Assuming that the same dynamic processes were active along the Azores Current, the eddy fluxes may contribute $1.2\times10^{13}\,\mathrm{W}$ to the heat budget of the eastern basin. Although its contribution to the total North Atlantic heat budget is fairly small, it shows the local importance of eddy heat transport in the vicinity of the Azores current. This current is only about 100 km wide, but it appears to be much wider on charts based on historical data. For example, OLBERS, WILLEBRAND and WENZEL (1982) report a zone of enhanced eastward surface flow between 31° and 36°N and 15° and 40°W (Fig. 16). A similar pattern is seen at 500 m, but with velocities slightly rotated to the left, a shift consistent with our calculations. This broad zone results from the meandering of the Azores Current.

The remarkable contrast north and south of 33°N is also found in potential vorticity maps of the North Atlantic. MCDOWELL, RHINES and KEFFER (1982) identify the wind driven gyre circulation with the region of homogeneous potential vorticity. The northern boundary is the surface outcrop of the 26.5 σ_θ contour in late winter which is located in our observational area (cf. SARMIENTO, RAOTH and ROETHER, 1982). Since meridional heat flux corresponds

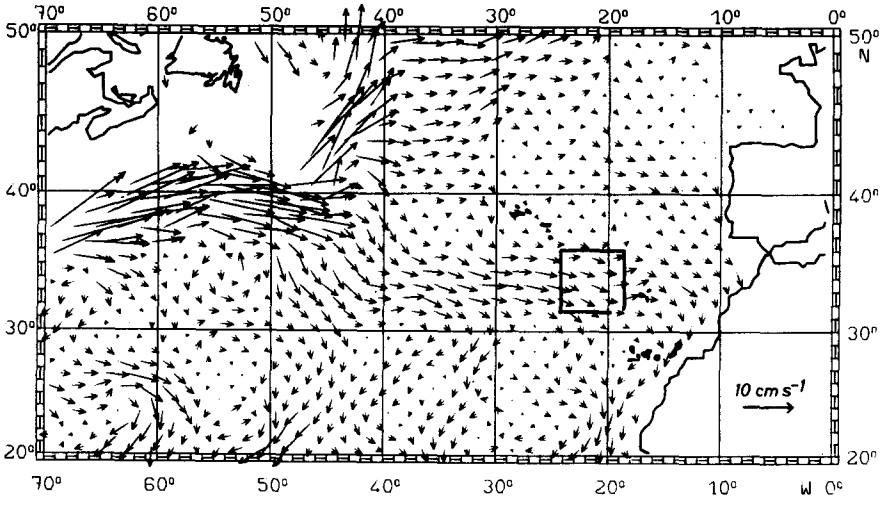

FIG. 16. North Atlantic mean surface flow as obtained from historical density data by diagnostic modelling (OLBERS *et al.*, 1982). The Azores Current appears to be much wider in the figure due to the extensive meandering as revealed by the *Poseidon* 86 measurements [Experimental site marked by frame, see also Fig. 2(b)].

to potential vorticity mixing, fluid enters and exits the wind-driven gyre in the vicinity of the meandering Azores Current.

Improvement in our understanding of the northward transport of heat in the upper waters of the eastern North Atlantic requires additional measurements. First, more meridional sections are needed to resolve the zonal characteristics of the mean flow field. Second, more zonal, high-spatial-resolution transects are needed to determine the eddy contributions to the northward heat flux. The present investigation has demonstrated the utility of combined towed and station observations. Each samples the environment differently in time and space, and each emphasizes different aspects of the flow and property distributions. When combined, the independent methods yield similar results for the primary aspects of the variability and, thereby, increase confidence in the interpretation of the data. For future experiments it is suggested that measurements be made on small enough spatial scales to resolve the energy-containing band of the $v'T'$ cospectrum. It is unlikely that such finescale resolution can be achieved using CTD observations, but towed and expandable techniques can be used to extend the spatial resolution. The agreement found between the XBT transects and XCP profiles is an example of the utility of combined, finescale observations. In the future it is vital to concentrate more measurements in the frontal or meander zone. Clearly, there is much interesting activity going on in this area, and some of this activity is in processes that are not generally regarded as important or even existent.

Acknowledgements—We thank two anonymous reviewers for their valuable suggestions on the original manuscript.

This work was funded by the Deutsche Forschungsgemeinschaft, Bonn-Bad Godesberg (SFB 133) and by NOAA grant NA81AA-D-00078.

REFERENCES

ARMI, L. and H. STOMMEL (1983) Four views of a portion of the North Atlantic Subtropical Gyre. *Journal of Physical Oceanography*, **13**(5), 828–857.

BRETHERTON, F. P., R. E. DAVIS and C. B. FANDRY (1976) A technique for objective analysis and design of oceanographic experiments applied to MODE-73. *Deep-Sea Research*, **23**, 559–582.

BRYDEN, H. (1976) Horizontal advection of temperature for low-frequency motions. *Deep-Sea Research*, **23**, 1165–1174.

BRYDEN, H. (1979) Poleward heat flux and conversion of available potential energy in Drake Passage. *Journal of Marine Research*, **37**, 1–22.

BRYDEN, H. and M. HALL (1980) Heat transport by currents across 25°N latitude in the Atlantic Ocean. *Science*, **207**, 884–886.

BUNKER, A. and L. V. WORTHINGTON (1976) Energy exchange charts of the North Atlantic Ocean. *Bulletin of the American Meteorological Society*, **57**, 670–678.

DANTZLER, H. L., Jr. (1977) Potential energy maxima in the tropical and subtropical North Atlantic. *Journal of Physical Oceanography*, **7**, 512–519.

DEFANT, A. (1961) *Physical oceanography*. Vol. 1, Pergamon, New York, 729 pp.

DICKSON, R. R. (1983) Global summaries and intercomparisons: Flow statistics from long-term current meter moorings. In: *Eddies in marine science*, A. R. ROBINSON, editor, Springer-Verlag, Berlin, 278–353.

DIETRICH, G., K. KALLE, W. KRAUSS and G. SIEDLER (1975) *Allgemeine Meereskunde*, Gebr. Borntraeger, Berlin, 513 pp.

DREVER, R. G. and T. B. SANFORD (1980) An expendable temperature and velocity profiler (XTVP). Near Surface Ocean Technology Workshop Proceedings, Naval Ocean Research and Development Activity, NSTL Station, MS, 163–173.

EMERY, W. J. (1983) On the geographical variability of the upper level mean and eddy fields in the North Atlantic and North Pacific. *Journal of Physical Oceanography*, **13**, 269–291.

EMERY, W. J. and J. S. DEWAR (1982) Mean temperature–salinity, salinity–depth and temperature–depth curves for the North Atlantic and the North Pacific. *Progress in Oceanography*, **11**, 219–305.

GARRETT, C. J. R. (1979) Mixing in the ocean interior. *Dynamics of the Atmosphere and Oceans*, **3**, 239–265.

GOULD, W. J. (1985) Physical oceanography of the Azores front. *Progress in Oceanography*, **14**, pp 167–190.

HALL, M. and H. BRYDEN (1982) Direct estimates and mechanisms of ocean heat transport. *Deep-Sea Research*, **29**(3A), 339–359.

HILLER, W. and R. H. KÄSE (1983) Objective analysis of hydrographic data sets from mesoscale surveys. *Berichte aus dem Institut für Meereskunde, Kiel*, **116**, 78 pp.

JOYCE, T. M., W. ZENK and J. M. TOOLE (1978) The anatomy of the antarctic Polar Front in the Drake Passage. *Journal of Geophysical Research*, **83**, 6093–6113.

KÄSE, R. H. and J. RATHLEV (1982) CTD-data from the North Canary Basin – *Poseidon* Cruise 86/2 26 March–13 April, 1982. *Berichte aus dem Institut für Meereskunde, Kiel*, **103**, 130 pp.

KÄSE, R. H. and G. SIEDLER (1982) Meandering of the subtropical front southeast of the Azores. *Nature*, **300**(5889), 245–246.

KEFFER, T. and P. P. NIILER (1982) Eddy convergence of heat, salt, density and vorticity in the subtropical North Atlantic. *Deep-Sea Research*, **29**, 201–216.

KNOLL, M., W. ZENK and E. BAUER (1982) Some XBT-observations on the thermal structure of the Warmwassersphäre in equatorial and lower latitudes of the eastern Atlantic. *D. hydrographische Zeitschrift*, **35**, 73–81.

KRAUSS, W. and R. H. KÄSE (1984) Mean circulation and eddy kinetic energy in the eastern North Atlantic. *Journal of Geophysical Research* (in press).

KRAUSS, W. and J. MEINCKE (1982) Drifting buoy trajectories in the North Atlantic Current, *Nature*, **296**(5859), 737–740.

KROEBEL, W. (1973) Die Kieler Multisonde. Ein Gerät zur *in situ*-Messung von Temperatur, Leitfähigkeit, Salzgehalt, Schallgeschwindigkeit und lichtoptischer Attenuation mit ersten Ergebnissen der *Meteor*-Fahrt Nr. 23 (1971) westlich von Gibraltar. *"Meteor" Forsch.-Ergebn.*, **A12**, 53-67.

LEETMAA, A. and A. F. BUNKER (1978) Updated charts of the mean annual wind stress, convergences in the Ekman layers, and Sverdrup transports in the North Atlantic. *Journal of Marine Research*, **36**, 311–322.

LEETMAA, A., P. P. NIILER and H. STOMMEL (1977) Does the Sverdrup relation account for the mid-Atlantic circulation? *Journal of Marine Research*, **35**, 1–10.

MANGELSDORF, P. C. (1962) The World's longest salt bridge. In: *Marine sciences instrumentation*, Vol. 1, Plenum Press, 173–185.

MCCARTNEY, M. S. (1982) The subtropical recirculation of mode waters. *Journal of Marine Research,* **40** (Suppl.), 427–464.

MCDOWELL, S., P. RHINES and T. KEFFER (1982) North Atlantic potential vorticity and its relation to the general circulation. *Journal of Physical Oceanography,* **12**, 1417–1436.

MCWILLIAMS, J. C. (1983) On the mean dynamical balances of the Gulf Stream recirculation zone. *Journal of Marine Research* (submitted).

MCWILLIAMS, J. C. and COLLABORATORS (1983) The local dynamics of eddies in the western North Atlantic. In: *Eddies in Marine Science*, A. R. ROBINSON, editor, Springer-Verlag, Berlin, 92–113.

MODE GROUP, THE (1978) The Mid-Ocean Dynamics Experiment. *Deep-Sea Research,* **25**, 859–910.

MÜLLER, T. and W. ZENK (1983) Eulerian current observations and XBT sections from the North East Atlantic, October 1980–March 1982, *Bericht des Instituts für Meereskunde, Kiel*, Nr. **114**, 145 pp.

NIILER, P. P. and J. STEVENSON (1982) The heat budget of tropical ocean warm-water pools. *Journal of Marine Research,* **40** (Suppl.), 465–480.

OLBERS, D. J., J. WILLEBRAND and M. WENZEL (1982) *Ocean Modelling* 1982, **46**, (unpublished manuscript).

OWENS, W. B., J. R. LUYTEN and H. L. BRYDEN (1982) Moored velocity measurements on the edge of the Gulf-Stream recirculation. *Journal of Marine Research,* **40** (Suppl.), 509–524.

PEDLOSKY, J. (1979) *Geophysical fluid dynamics.* Springer-Verlag, New York, 624 pp.

POLLARD, R. T. and S. PU (1985) Structure and ventilation of the upper Atlantic Ocean northeast of the Azores. *Progress in Oceanography,* **14**, 443–462.

SANFORD, T. B. (1971) Motionally induced electric and magnetic fields in the sea. *Journal of Geophysical Research,* **76**(15), 3476–3492.

SANFORD, T. B., R. G. DREVER, J. H. DUNLAP and E. A. D'ARARO (1982) Design, Operation and performance of an expendable temperature and velocity profiler (XTVP), APL-VW 8110, Applied Physics Laboratory, University of Washington, 83 pp.

SANFORD, T. B. and P. F. SPAIN (1982) Meteor-Cruise 57: Scientific Results, APL-UW 8213, Applied Physics Laboratory, University of Washington, 40 pp.

SARMIENTO, J. L., C. G. H. ROOTH and W. ROETHER (1982) The North Atlantic Tritium distribution in 1982, *Journal of Geophysics,* **687**, 8047–8056.

SIEDLER, G. and L. STRAMMA (1983) The applicability of the *T/S* method to geopotential anomaly computations in the Northeast Atlantic. *Oceanologica Acta,* **8**(2), 167–172.

STOMMEL, H., P. P. NIILER and D. ANATI (1978) Dynamic topography and recirculation of the North Atlantic. *Journal of Marine Research,* **36**, 449–468.

STRAMMA, L. (1981) Die Bestimmung der dynamischen Topographie aus Temperaturdaten aus dem Nordostatlantik. *Berichte aus dem Institut für Meereskunde, Kiel,* Nr. 84, 66 pp.

VON ARX, W. S. (1950) An electromagnetic method for measuring the velocities of ocean currents from a ship under way. *Papers in Physical Oceanography and Meteorology,* **11**(3), 62 pp.

VOORHIS, A. D., E. H. SCHROEDER and A. LEETMAA (1976) The influence of deep mesoscale eddies on surface temperature in the North Atlantic subtropical convergence. *Journal of Physical Oceanography,* **6**, 953–961.

WARREN, B. A. (1972) Insensitivity of subtropical mode water characteristics to meteorological fluctuations. *Deep-Sea Research,* **19**, 1–19.

WILLEBRAND, J. and J. MEINCKE (1980) Statistical analysis of fluctuations in the Iceland–Scotland frontal zone. *Deep-Sea Research,* **27A**, 1047–1066.

WORTHINGTON, V. (1959) The 18°-water in the Sargasso Sea. *Deep-Sea Research,* **5**, 297–305.

WUNSCH, C. (1980) Meridional heat flux of the North Atlantic Ocean. *Proceedings National Academy of Science USA,* 77 (9), 5043–5047.

WUNSCH, C. (1981) Low-frequency variability of the sea. In: *Evolution of physical oceanography,* B. A. WARREN and C. WUNSCH, editors, MIT Press, Cambridge, 623 pp.

WUNSCH, C. and B. GRANT (1982) Towards the general circulation of the north Atlantic Ocean. *Progress in Oceanography,* **11**, 1–59.

WÜST, G. (1935) Schichtung und Zirkulation des Atlantischen Ozeans. Die Stratosphäre. In: Wissenschaftliche Ergebnisse der Deutschen Atlantischen Expedition auf dem Forschungs und Vermessungsschiff "Meteor" 1925–1927, 6. Lieferung 1. Teil, 2, 180 pp (The stratosphere of the Atlantic Ocean, W. J. EMERY, editor, 1978, Amerind, New Delhi, 112 pp.)

WYRTKI, C., L. MAGAARD and J. HAGER (1976) Eddy energy in the oceans. *Journal of Geophysical Research,* **81**, 2641–2646.